Stem Cells Transl Med. Author manuscript; available in PMC 2017 January 01.

Published in final edited form as:
Stem Cells Transl Med. 2016 July ; 5(7): 946–959. doi:10.5966/sctm.2015-0282.

Embryological Origin of Human Smooth Muscle Cells Influences Their Ability to Support Endothelial Network Formation

Johannes Bargehr[#], **Lucinda Low**[#], **Christine Cheung**, **William G Bernard**, **Dharini Iyer**, **Martin R Bennett**, **Laure Gambardella**, and **Sanjay Sinha**
The Anne McLaren Laboratory for Regenerative Medicine, West Forvie Building, Forvie Site, University of Cambridge, Robinson Way, Cambridge CB2 0SZ,UK

Division of Cardiovascular Medicine, University of Cambridge, ACCI Level 6, Box 110, Addenbrooke's Hospital, Hills Road, Cambridge CB2 0QQ, UK

[#] These authors contributed equally to this work.

Abstract

Objective—Vascular smooth muscle cells (SMCs) from distinct anatomic locations derive from different embryonic origins. Here we investigated the respective potential of different embryonic origin-specific SMCs derived from human embryonic stem cells (hESCs) to support endothelial network formation *in vitro*.

Methods and Results—SMCs of three distinct embryological origins were derived from an mStrawberry-expressing hESC line and were co-cultured with GFP-expressing human umbilical vein endothelial cells (HUVEC) to investigate the effects of distinct SMC subtypes on endothelial network formation. Quantitative analysis demonstrated that LM-derived SMCs best supported HUVEC network complexity and survival in 3D co-culture in matrigel. The effects of the LM-SMCs on HUVECs were at least in part paracrine in nature. A TaqMan Array was performed to identify possible mediators responsible for the differential effects of the SMC lineages and a microarray to determine lineage-specific angiogenesis gene signatures. Midkine (MDK) was identified as one important mediator for the enhanced vasculogenic potency of LM-SMCs. The functional effects of MDK on endothelial network formation were then determined by siRNA-mediated knockdown in SMCs, which resulted in impaired network complexity and survival of LM-derived SMC co-cultures.

Corresponding Author: Dr. Sanjay Sinha, The Anne McLaren Laboratory for Regenerative Medicine, West Forvie Building, Forvie Site, University of Cambridge, Robinson Way, CB2 0SZ Cambridge, UK, Tel.: +44 1223 747479, Fax: +44 1223 763350. ss661@cam.ac.uk.

Author Contribution:
Johannes Bargehr: Conception and design, collection and/ or assembly of data, data analysis and interpretation, manuscript writing
Lucinda Low: Conception and design, collection and/ or assembly of data, data analysis and interpretation
Christine Cheung: Conception and design, provision of study material or patients
William G Bernard: Data analysis and interpretation
Dharini Iyer: Administrative support, data analysis and interpretation
Martin R Bennett: Administrative support, data analysis and interpretation
Laure Gambardella: Data analysis and interpretation
Sanjay Sinha: Conception and design, financial support, administrative support, data analysis and interpretation, final approval of manuscript

[7]**Disclosures**
There is nothing to declare.

Europe PMC Funders Author Manuscripts

Conclusions—This is the first study to show that SMCs from distinct embryonic origins differ in their ability to support HUVEC network formation. LM-derived SMCs best support endothelial cell network complexity and survival *in vitro,* in part through increased expression of MDK. A lineage-specific approach may be beneficial for vascular tissue engineering and therapeutic revascularisation.

Keywords

Embryological Origin; Lineage specific; Smooth Muscle Cells; Endothelial Cells; Network Formation

1 Introduction

Mural cells are essential for the stabilisation and maturation of new endothelial cell networks (1–3). In human embryonic development, nascent vascular networks emerge through vasculogenesis and angiogenesis. Subsequent stabilisation and maturation of this network is achieved through recruitment of mural cells, involving pathways such as the platelet-derived growth factor-BB (PDGF-BB) and transforming growth factor beta (TGF-β) (4). The critical role of mural cells has been demonstrated in PDGF-BB deficient mice, which developed capillary microaneurysms in the absence of mural cells (3). Furthermore abnormal vascular morphogenesis, including changes in microvessel architecture, endothelial cell quantity and morphology, and transendothelial permeability, has been described in PDGF-BB and PDGF-Rβ deficient mice (5).

Both cell-cell and paracrine mechanisms are thought to regulate vessel maturation but remain poorly characterised (6, 7). In particular, relatively little is known about the effect of the developmental origins of mural cells on their signalling to endothelial cells and how this affects vessel development. Mural cells have a variety of embryonic origins, which may affect their functional abilities (8, 9). In chick embryos, isolated smooth muscle cells (SMC) from the neural crest and from the mesoderm exhibit different growth and transcriptional responses to TGF-β (10). Historic *in vivo* data from chick embryos shows that SMC responses are not environment- but lineage-specific. These experiments demonstrated that SMCs derived from the nodose placode had a superior ability to replace ablated cardiac neural crest SMCs when compared to those of mesodermal origin, corroborating the presence of lineage-specific functionality in different SMC populations (11).

Regenerative cardiovascular medicine is making rapid progress in the treatment of ischaemic or dysfunctional tissues through direct cell injection as well as tissue engineered constructs. Adequate vascularisation of cellular grafts after transplantation is critical for long term perpetuation of homeostasis and functionality for which mural cells are paramount. However to date this topic remains poorly addressed and translational approaches would benefit substantially from a better understanding of mural cell functionality. Furthermore it remains unknown how the embryonic origin of hESC-derived SMCs influences vascular network development and what the signalling events involved in this process are. We have previously generated a model of lineage-specific SMC development from human embryonic stem cells (hESC) or human induced pluripotent stem cells (iPSC), allowing for derivation of mural

Europe PMC Funders Author Manuscripts

cells from the lateral mesoderm (LM), the paraxial mesoderm (PM) and the neuroectoderm (NE) (12).

Here we report for the first time that endothelial network formation is substantially determined by the embryonic origin of smooth muscle cells. Gene expression profile and microarray data exhibit a distinct up-regulation of angiogenesis- or vasculogenesis-related genes in LM-derived SMCs. We elucidate the functional role of midkine (MDK) as one mediator of this effect and demonstrate that an siRNA-mediated knockdown results in substantially impaired vascular network formation in LM-derived SMC co-cultures.

2 Experimental Procedures

2.1 hESC culture and differentiation

hESCs (H9, WiCell, Madison) were maintained in a chemically defined medium (CDM-BSA) containing Activin-A (10 ng/ml, R&D Systems) and FGF2 (12 ng/ml, R&D Systems) as previously described (13). Chemically defined medium consisted of IMDM (250 ml, Life Technologies), Ham's F12 (250 ml, Life Technologies), Pen/Strep (5 ml, Life Technologies), Insulin (350 µl, Roche), Transferin (250 µl, Roche), chemically defined 100x lipid concentrate (5 ml, Life Technologies) and monothioglycerol (20 µl, Sigma). Differentiation to intermediate lineages and smooth muscle cells was performed as previously described in CDM-PVA, containing polyvinyl alcohol (PVA, 1 mg/ml, Sigma)(14). In brief, early mesoderm differentiation was started with a combination of CDM-PVA, FGF2 (20 ng/ml), LY294002 (10 µM, Sigma) and BMP4 (10 ng/ml, R&D) for 1.5 days. Consequently either lateral mesoderm differentiation was started in CDM-PVA, FGF2 (20 ng/ml) and BMP4 (50 ng/ml) for 3.5 days or paraxial mesoderm differentiation in CDM-PVA, FGF2 (20 ng/ml) and LY294002 (10 µM) for 3.5 days. To induce neuroectoderm differentiation, cells were cultured in CDM-PVA, FGF (12 ng/ml) and SB431542 (10 µM, Tocris) for 7 days. For smooth muscle cell differentiation, LM-, PM- and NE-cells were resuspended as single cells in CDM-PVA, PDGF-BB (10 ng/ml, Peprotech) and TGF-β1 (2 ng/ml, Peprotech) for 6 days.

2.2 Generation of mStrawberry-expressing hESCs

A lentiviral-based vector was used to allow the transduction of two reporter genes, encoding luciferase and the fluorochrome mStrawberry, driven by the constitutively active CAGGS promoter. To produce a transduced hES cell line, P64 H9 hESCs were passaged 24 hours prior to lentiviral transduction and plated onto gelatine (0.1%) coated 6 well plates. Lentiviral transduction was carried out by addition of polycation protamine sulphate (10 µg/ml) and lentivirus at an MOI of 5, or polycation protamine sulphate alone as a negative control, to approximately $2x10^5$ cells maintained in CDM with ActivinA (10 ng/ml) and FGF2 (12ng/ml). Cells were maintained in culture media for 48 hours and the media was changed daily. 24 hours prior to dissociating transduced cells, the culture media was supplemented with 10 µM Rho kinase inhibitor (Y-27632, Tocris). 72 hours after transduction, cells were incubated in TrypLE Express (Invitrogen) for 5 minutes at 37°C, and then dissociated by gentle pipetting. Cells were plated onto a 10cm plate that had been coated with 0.1% porcine gelatine and contained $1x10^5$ irradiated mouse embryonic

fibroblasts as feeder cells (feeder). Cells were maintained in DMEM/F12 medium, containing 20% knockout serum replacement and FGF2 (4ng/ml) supplemented with Rho kinase inhibitor (10 μM). Colonies that appeared were allowed to expand over a 7-day time period. Successfully transduced colonies were identified by fluorescence microscopy, picked, and expanded until a stable lentiviral luciferase mStrawberry (LVLS) reporter hES cell line was able to be maintained in a feeder free culture system utilising the chemically defined medium as described previously.

2.3 Generation of GFP-expressing HUVECs

A lentiviral-based vector was used to allow the transduction of reporter gene, EGFP, driven by the constitutively active EF-1alpha promoter. To produce GFP-expressing HUVECs, P6 HUVECs were passaged 24 hours prior to lentiviral transduction and plated onto T75 flask that had been coated with 0.1% porcine gelatine. Lentiviral transduction was carried out by addition of polycation protamine sulphate (10 μg/ml) and lentivirus at an MOI of 10, or polycation protamine sulphate alone as a negative control, to approximately $5x10^5$ cells maintained in human large vessel endothelial cell growth medium (Cellworks, Buckingham, UK). Cells were maintained in culture media for 48 hours after transduction and the media was changed daily. This protocol produced a HUVEC cell line with 99.5% GFP+ cells, as determined by flow cytometry.

2.4 qRT-PCR

Total RNA extraction was performed using the GenElute Mammalian Total RNA Miniprep Kit (Sigma) and 250 ng of RNA converted to complementary DNA (cDNA) by reverse transcription using Maxima First Strand cDNA Synthesis Kit (ThermoFisher) as per the manufacturer's instructions. qRT-PCR reactions were performed with Applied Biosystems 7900HT Fast Real-Time PCR System using FAST SYBR Green Master Mix (ThermoFisher) and primers of the target genes. Obtained values were normalized to the housekeeping genes *GAPDH* and *PBGD* in the same run. Primer sequences are depicted in the Supplementary material online, Methods (Table S1).

2.5 Immunocytochemistry

Cells were fixed in 4% Paraformaldehyde (PFA) and permeabilised with 0.5% Triton X-100 /PBS. This was followed by blocking in 3% BSA/PBS for 45 minutes, at room temperature. Primary antibody incubations were performed at 4°C overnight. After incubation with primary antibody, cells were washed and incubated with Alexa-Fluor Conjugated secondary antibodies for 45 minutes at room temperature. Finally cells were stained with DAPI for 10 minutes to visualize the nuclei. Images were acquired on a Zeiss LSM700 using ZEN software. A detailed description of antibodies and dilutions used is provided in the Supplementary material online, Methods (Table S2).

2.6 ELISA

For ELISA of D6 PT smooth muscle cell supernatant, Human Midkine ELISA Development Kit (Peprotech) was used as per the manufacturer's instructions. Plate readings were

obtained on a 2030 Multilabel Reader (VICTOR X3, Perkin Elmer/Caliper Life Sciences, Hopkinton, MA, USA).

2.7 3D co-cultures

A schematic of this procedure is presented in supplementary figure 1, panel A. GFP-HUVECs and D6 PT SMCs derived from mStrawberry H9's were dissociated, centrifuged and resuspended in warm CDM-PVA. Cells were counted and cell combinations were prepared in 15 ml falcon tubes, containing either $1.6x10^5$ HUVECs alone, or a combination of $1.6x10^5$ HUVECs and $3.2x10^4$ SMCs (ratio 5:1). Cell mixtures were then centrifuged and resuspended in 18 μl ice-cold HUVEC media (TCS Cellworks, Cat# M-2953). Tubes were spun down, the supernatant aspirated and resuspended in 18 μl ice cold HUVEC media. Subsequently, 20 μl of ice cold Matrigel was added and mixed with the cell suspension. Finally 10 μl of each sample were added to each well of a pre-chilled Ibidi Angiogenesis μ-Slide (Ibidi, Cat# 81506), in technical triplicates. The slide was incubated for 45 minutes at 37°C before adding (volume) warm HUVEC media to each well. Media was refreshed every second day throughout the experiment.

2.8 3D paracrine assay

A schematic of this procedure is presented in supplementary figure 1, panel B. For paracrine 3D co-cultures the 8 outer wells of each 9-well section of 2 Ibidi 2x9 well μ-slides were coated with Matrigel and incubated at 37°C for 30 minutes. GFP-HUVECs and D6 PT SMCs derived from mStrawberry H9's were dissociated, centrifuged, and resuspended in CDM-PVA. Cells were counted ($6.4x10^5$ HUVECs or $1.35x10^5$ SMCs) and were transferred to separate 15 ml falcon tubes and centrifuged. HUVECs were resuspended in 78 μl ice cold HUVEC media and mixed with 80 μl ice cold Matrigel. 32 μl of HUVEC suspension were added to the middle wells of the 2x9 well Ibidi μ-slide. Each SMC sample was resuspended in 540 μl warm HUVEC media and 60 μl were added to each of the 8 outer wells of the μ-slide. For the HUVEC alone sample, media containing no cells was added to the 8 outer wells. The slide was incubated for an hour at 37°C to allow the cells to attach and Matrigel to solidify. Following this the media was aspirated form all the SMC wells of the μ-slide and the chamber was filled with 600 μl of warm endothelial media. Media was refreshed every second day throughout the experiment.

2.9 Confocal Microscopy

For co-cultures and paracrine assays, images were acquired in technical triplicates per each biological replicate. For the siRNA-mediated knockdown of MDK, quantification was further optimised. Three images were taken per each technical replicate, corresponding to 9 images per biological replicate per condition. Images were obtained on a Zeiss LSM700 using ZEN software.

2.10 Image quantification and analysis

For quantification, three technical replicates, consisting of one image each, were analysed per biological replicate. Lsm files were analysed in a blinded fashion with ImageJ. For total network area, the images were converted to binary images and the threshold was set until

exclusive visualization of the network area was obtained. Values obtained reflect μm^2. For quantification of total cord length lines were manually drawn on the network, their length measured and values converted to μm. Branch points were counted manually after transformation of all files into binary images. Data presented as bar charts consist of three independent biological replicates, each of which is the average of three analysed images (technical replicates).

2.11 TaqMan Array

cDNA was synthesized from total RNA samples as described for qRT-PCR. For PCR amplification the TaqMan® master mix was combined with the cDNA, loaded on the TaqMan® plate and ran, using Applied Biosystems 7900HT Fast Real-Time PCR System.

2.12 Microarray analysis

The genes analysed in the TaqMan Human Angiogenesis Array were extracted from our previously performed microarray dataset on smooth muscle cells derived from lateral-plate mesoderm, paraxial mesoderm, and neuroectoderm after 12 days of PDGF-BB and TGF-β1 treatment (12). Heat maps of relative gene expression were generated with Perseus (MaxQuant, v1.4.1.3). Array datasets are available from the ArrayExpress microarray data repository under accession number E-MTAB-781.

2.13 siRNA-mediated knockdown of MDK

MDK silencer select siRNA was synthesized by Ambion Life Technologies (s8625). As a negative control, scrambled (scr) siRNA was used (Silencer Select negative control siRNA, Ambion). SMCs were transfected with 10nM siRNA twice, once on day 11 and once on day 12 (see Supplementary material online, Methods).

2.14 Statistical Analysis

Results are expressed as mean ± standard error of mean (SEM) of at least three biological replicates of independent experiments. Statistical comparisons were carried out using either Student's T Test for two groups of samples or one-way ANOVA with Bonferroni's post-hoc test in case of multiple group comparisons, using Graph Pad Prism Software. Measuring two-sided significance, p-values <0.05 were considered statistically significant.

3 Results

3.1 Generation of embryonic origin-specific intermediates and SMCs for a 3D co-culture with human umbilical vein endothelial cells (HUVECs)

We first generated mStrawberry-expressing hESCs and GFP-expressing HUVECs (Figure S1A and S1B). mStrawberry-expressing hESCs were differentiated to LM, PM and NE and subsequently treated with PDGF-BB and TGF-β1 (designated as PT) to induce SMC differentiation. On day 13 of the protocol, 3D matrigel co-cultures and paracrine assays were set up, in which HUVECs were used to model endothelial network formation. The respective potential of lineage-specific mural cells to support vasculogenesis was tested using embryonic origin-specific SMCs obtained following 6 days of differentiation in PT (Figure

1A). To validate that lineage-specific SMCs were generated and used for the matrigel vasculogenesis assays, lineage-specific marker expression was examined at the mRNA and protein levels. High expression of the LM markers *ISL1* and *NKX 2.5* was observed specifically in the LM population, as was the specific expression of the PM markers *PAX3* and *MEOX1* in PM (Figure 1B and 1C). Expression of NE markers *SOX1* and *GBX2* was seen preferentially in NE, as shown previously (Figure 1D). In accordance with the mRNA data, LM, PM and NE respectively and specifically expressed ISL1, PAX3 and SOX1 at the protein level, as shown by immunocytochemistry (Figure S2A-S2C). To show that SMCs were generated from the intermediate lineages, expression of SMC markers *ACTA2* and *CNN1* was demonstrated at the mRNA and protein level before the co-cultures were started (Figure 1E and S3A-3C). In conclusion, embryonic origin-specific SMCs were generated as shown by stage- and lineage-specific marker expression.

3.2 LM-derived SMCs best support HUVEC network formation in a 3D co-culture model

To investigate the effects of each SMC lineage on endothelial network formation, 3D co-cultures were performed (Figure S4A). To show that mural cells improve endothelial network stability as well as complexity, a HUVECs only assay was performed and compared to the other SMC groups. On day 4 of the co-culture protocol, LM-derived SMCs accounted for the best endothelial network formation as reflected by larger network area, higher total cord length and greater number of branch points, compared to PM- and NE-derived SMCs and HUVECs alone (Figure 2A). The effect of the differential ability of SMCs to support endothelial network complexity became first apparent on day 2, peaked on day 4 and could be observed throughout all time points until day 8. The absolute potential of SMCs to provide endothelial network stability became most evident on day 8, when the networks consisting of HUVECs alone had disintegrated entirely. As the difference in vasculogenic potency between the three lineages was best reflected on day 4, this time point was chosen for further endothelial network analysis and quantification. Self-assembly of SMCs and ECs was particularly robust in the LM-derived SMC group with the SMCs providing physical support through wrapping around the endothelial tubes (Figure 2B). Quantification of this effect demonstrated that LM-derived SMC co-cultures had the highest total endothelial network area on day 4 and on day 8, compared to the two other SMC lineages and to HUVECs alone (Figure 2C). Furthermore, endothelial networks supported by SMCs of the LM origin accounted for a higher total cord length and a higher number of branch points than networks co-cultured with the other two SMC lineages, at both time points (Figure 2D and 2E respectively).

To elucidate whether this effect was paracrine in nature, 3D paracrine assays were performed. HUVECs were plated in the central well of a 9 well chamber and SMCs in the adjacent 8 wells with walls separating the wells only half way to the top. This setup allowed for SMC conditioned media but not for SMCs to be in physical contact with the endothelial cells. Hence any effect in HUVEC network formation observed must be a paracrine but not cell-cell dependent effect (Figure S4B). At day 4 and day 8 of the co-culture timeline, LM-derived SMCs presented as the best supportive cell type for endothelial network formation (Figure 3A). Quantification of day 4 of the paracrine assay data showed that HUVECs co-cultured with LM-derived SMCs accounted for a greater total endothelial network area, with

a higher total cord length and more branch points than HUVECs co-cultured with SMCs of the two other lineages or HUVECs alone (Figure 3B - 3D). These results suggested that LM-derived SMCs best supported endothelial network formation and that this effect was at least partly paracrine in nature.

3.3 Midkine is one mediator of superior vascular network formation in LM-derived SMC co-cultures and is part of a unique angiogeneic expression pattern

To identify possible mediators of the LM-derived SMCs' differential ability to support vascular network formation, a TaqMan© Array Human Angiogenesis Panel was performed on D6 PT SMCs derived from LM, PM and NE. This assay allows the screening of 94 genes involved in human angiogenesis and lymphangiogenesis. After evaluation of all genes, the panel was narrowed down to nine candidates which exhibited a selective up-regulation in LM-derived SMCs but not in SMCs of PM or NE origin. These included: *AMOT, ANGPT1, ANGPTL2, VEGFC, FBLN5, ENPP2, MDK, SERPINF1* and *PTN* (Figure 4A). Validation of the Human Angiogenesis Panel was carried out by qRT-PCR and showed a statistically significant up-regulation of *AMOT, ANGPTL2, VEGFC, FBLN5* and *MDK* selectively in LM-derived SMCs. Compared to the other candidate genes, *MDK* showed the highest statistical significance, when comparing its expression in LM-derived SMCs against expression levels in PM- and NE-derived SMCs (Figure 4B). To further corroborate this data we analysed a microarray of D12 PT lineage-specific SMCs. The respective heat map is depicted in Figure 4C and includes all genes that accounted for an overall statistical significant difference between the three SMC lineages ($p<0.05$). The expression pattern visualised demonstrates that LM-derived SMCs up-regulate genes that are not expressed in PM- and NE-derived SMCs, thus comprising a list of genes that is uniquely confined to the embryonic origin of the LM lineage (Figure 4C). Analysis of the microarray including all of the 94 angiogenesis genes from the TaqMan Array was also performed (Figure S5). In summary, MDK was identified as one of 9 candidate genes that were selectively expressed in the LM-derived SMC lineage, which exhibits a lineage specific angiogenic expression pattern.

3.4 SMC-derived MDK regulates vascular network formation in LM-derived SMC and HUVEC co-cultures

To examine the role of MDK in vascular network formation, an siRNA-mediated knockdown was performed. MDK siRNA was added to the SMC cultures on day 11 and day 12 of the differentiation protocol, before starting the co-cultures with the knocked down SMCs on day 13 (Figure S6A). Confirmation of an efficient knockdown of MDK was demonstrated by qRT-PCR and ELISA. In line with the results from the TaqMan array, ELISA confirmed that MDK was also selectively expressed in LM-derived SMCs at the protein level (Figure S6B and S6C). Co-cultures of MDK-siRNA-treated SMCs with endothelial cells revealed substantial phenotypic changes in the LM-derived SMC co-cultures. Impaired MDK expression resulted in a significant decrease of the total endothelial network area of LM-derived SMC co-cultures over a continuous timeline of 4 days (Figure 5A). Extensive quantification of this effect revealed a significant decrease in the total endothelial network area of LM-derived SMC co-cultures over a time period of 4 days. As anticipated, no substantial differences in endothelial network formation were seen in co-

cultures with SMCs derived from the PM or NE (Figure 5B). Knockdown of MDK also resulted in a significant decrease in endothelial network complexity, as demonstrated by a significant decrease in total cord length as well as number of branch points (Figure 5C and 5D). To confirm our initial finding that LM-derived SMCs promote angiogenesis partly in a paracrine fashion, for which one mediator is MDK, we also performed paracrine co-cultures with the MDK siRNA treated SMCs. Over a time course of 4 days, MDK knockdown selectively impaired endothelial network formation in LM-derived SMC paracrine assays. Again no effect of MDK knockdown was seen in PM- and NE-derived SMC co-cultures (Figure 6A). Quantification of this effect on day 2 of the paracrine assays showed a significant decrease in total endothelial network area and total cord length in the LM-derived SMC group (Figure 6B and 6C). Similar to the effect observed in 3D co-cultures, endothelial network complexity in the paracrine assay was also decreased, as demonstrated by the decreased number of branch points (Figure 6D).

Finally, to examine whether MDK alone in isolation from other angiogenic factors produced by SMCs was able to promote human vasculogenesis, 3D matrigel cultures with HUVECs and recombinant MDK were performed (Figure 7A). Endothelial networks supplemented with recombinant MDK (5000pg/ml) accounted for larger and more complex networks, including a higher total cord length and a higher number of branch points than HUVECs alone. This finding corroborates the importance of this angiogenic factor in vascular network formation (Figure 7B to 7D). Collectively, this data shows that MDK is an important factor in the selective ability of LM-derived SMCs to support human vasculogenesis, promoting not only network size but also complexity.

4 Discussion

Microvascular network formation has not been devoted major scientific attention in regenerative cardiovascular research. However, recent attempts to regenerate ischemic tissue render this field highly relevant for the generation of functional tissue grafts *in vitro* and *in vivo*. We show for the first time that the embryonic origin of mural cells has a functional impact on developing microvascular networks, which has implications for regenerative cardiovascular medicine. Specifically, we demonstrated that LM-derived SMCs provide superior support to endothelial network formation, compared to SMCs originated from the PM or NE. Importantly, microarray and gene expression data identified MDK as one mediator of this effect, confirmed by loss- and gain-of-function studies.

Regenerative medicine has made remarkable progress in its endeavours to regenerate ischaemic and dysfunctional body tissues. In the cardiovascular system it has been demonstrated that transplantation of hESC-derived cardiomyocytes leads to re-muscularization, electrical coupling and partial restoration of cardiac function up to 4 weeks post transplantation in rodents (15, 16). More recently heroic efforts in the Murry lab have demonstrated that transplantation of 1 billion cardiomyocytes results in robust muscular grafts of infarcted non-human primate hearts (17). However for establishment of physiological homeostasis and long term maintenance of graft function, efficient vascularisation is likely to be necessary, particularly given that oxygenation by diffusion is only sufficient for grafts that are 4-7 cell layers (~100 um) thick (18). Similar reservations

apply for tissue-engineered cardiac constructs which have shown to promote cardiac function after epicardial transplantation to rat hearts in the short term (19). Indeed several studies have shown that vascularisation promotes cardiac graft development and maturation (20, 21). However, the potential for vascularisation to support regenerative medicine applications will only be realised through a deeper understanding of the ability of different cell types to contribute to vasculogenesis, angiogenesis and ultimately arteriogenesis.

Relatively little is known to date about the embryonic origin of mural cells in microvascular development. Pericytes comprising the microvasculature of lung, liver and gut have been tracked back to mesenchymal origin (22–24) while coronary pericytes originate from the epicardium (25, 26), which is a lateral plate mesoderm derivative. In contrast, those composing the micro-cerebrovasculature and the thymus derive from the neural crest (27, 28). A number of investigators have shown lineage-dependent functional differences for SMCs comprising large vessels. For NE-derived SMCs a functional lineage specific response was shown after Angiotensin II treatment (29) and differentiation of this lineage revealed myocardin-related transcription factor B (MKL2) as *sine qua non* (10). However it remains unknown whether lineage-specific effects of mural cells exist in microvascular development. Due to the high prevalence and rising incidence of diseases involving pathologies in the microvasculature, it is of great interest to elucidate the nature and mediators of lineage specific effects in endothelial network formation. Furthermore this information might aid attempts to revascularise ischemic body tissues and to bioengineer tissue constructs for regenerative purposes.

Searching for possible mediators of the ability of LM-derived SMCs to better support vascular network formation, we made use of a TaqMan Array Human Angiogenesis Panel. Validation of this assay by qRT-PCR revealed that MDK was one of five genes that showed a statistically significant up-regulation in LM-derived SMCs. MDK is a well-studied target in oncology with a direct correlation of its expression levels and microvessel density in salivary gland tumours and oral squamous cell carcinomas (30, 31). An MDK transfected Breast Carcinoma Cell line was reported to exhibit a greater vascular density and a higher tumor and endothelial cell proliferative index compared to a mock-transfected control cell line (32). In line with these findings it has been shown that high expression levels in patients with invasive bladder cancer correlate with poor survival (33).

In our human *in vitro* system, knockdown of MDK resulted in significantly impaired vascular network formation. Suggesting a role in angiogenesis, MDK-deficient mice have been shown to exhibit less lung metastasis of Lewis lung carcinoma cells and reduced tumorigenesis of neuroblastomas (34, 35). In the cardiovascular field, MDK injection, as well as MDK gene transfer, into post-infarcted rat hearts has been demonstrated to decrease cardiac remodelling through anti-apoptotic and pro-vasculogenic effects (36, 37). However, these studies investigated the formation of endothelial cell networks without taking into account the effect of mural cells. In addition, it has not yet been demonstrated that SMCs and their embryonic origins play key roles in the production of this cytokine. Our model is the first of its kind that provides an important insight into the functional role of MDK during embryonic vascular development in a human system.

Here we have also shown that support through LM-derived SMCs results in a more developed endothelial network, reflected in a higher number of branch points. Of note, knockdown of MDK resulted in fewer vascular branch points and supplementation of recombinant MDK supported network formation in HUVEC monocultures similar to those seen in LM-derived SMC co-cultures. These results indicate that MDK is involved in generating a complex, branched endothelial network. At the same time HUVECs alone appear to form larger and less complex endothelial cords. In the context of vascular network formation, the role of VEGF and Notch in tip and stalk cell specification and vascular patterning has extensively been described, but the role of MDK remains unknown (38–43).

In the current study we have provided microarray data of lineage-specific D12 PT SMCs and shown that the three SMC lineages account for individual angiogenic gene expression signatures. While our 3D endothelial network formation assay focuses on early vascular development by using D6 PT SMCs, we were able to coherently show that more mature SMCs express the same genes as on D6 of SMC differentiation with PT and additionally up-regulate others by D12. This Taqman array and microarray provide a valuable library of targets to study in the context of vascular network formation. Thus, other putative mediators of the beneficial effects of LM-derived SMC on endothelial network formation include Angiomotin (AMOT), Angiopoietin-like protein 2 (ANGPTL2), Fibulin 5 (FBLN5) and Vascular endothelial growth factor C (VEGF-C).

In the current study we have chosen matrigel to study the effects of mural cells on endothelial network formation. At the same time we wanted to elucidate key signals responsible for the differential ability of embryonic origin specific SMC lineages to allow for superior survival and growth of more complex endothelial networks. Matrigel assays are a widely used tool to study EC network formation and EC-mural cell crosstalk and are used as such by leading vascular laboratories around the world (44–48). In this context matrigel has been well established as a cord forming assay. While there are limitations regarding lumen formation the main objective of this study was to investigate branching and survival in a 3D context, which was well served by the system used. Of note we demonstrated that LM-derived SMC also allow for growth of more complex endothelial networks with a higher number of branch points, which is not a mere consequence of superior survival but a reflection of the angiogenic effect of MDK, which was confirmed by loss and gain of function studies.

The fact that LM-derived SMCs exhibit the best supportive function is not surprising because they emerge from a unique embryonic origin and express different sets of genes that are implicated in vasculogenesis. Whether these observations have an impact *in vivo* is a question that has to date not been addressed. In this regard it would be of interest to evaluate the vasculogenic potential of lineage-specific SMCs in a wound healing assay *in vivo*.

While this study is the first to demonstrate that the lineage specificity of mural cells has a functional impact on developing endothelial networks, it remains to be seen how endothelium from different vascular beds interacts with smooth muscle cells of different types. Recent studies have shown that endothelial cells from different vascular territories display unique properties and indeed these different endothelial cell populations have been

demonstrated to have unique, tissue specific signatures (49). However, it is unclear how these signatures are obtained; either through different intermediate developmental steps taken by the angioblasts, or a direct effect of the tissue specific microenvironment. Further studies should investigate how to generate tissue specific endothelial cells and whether these show distinct responses to the lineage-specific SMCs we have established. In this regard one future endeavour of tissue engineering and regenerative medicine will be the generation of embryonically and physiologically relevant body tissues in which lineage specific vascular cells will play a key role.

5 Conclusion

Taken collectively we have demonstrated that the embryonic origin of mural cells has a functional impact in endothelial network development, complexity and survival for which MDK is one important mediator. Fully exploiting the lineage-specific functionality of mural cells may prove critical for vascular tissue engineering and therapeutic revascularisation.

Supplementary Material

Refer to Web version on PubMed Central for supplementary material.

Acknowledgements

We are grateful to Dr. Helle Jorgenson (University of Cambridge) for discussions and Donna Leaford (Wellcome Trust MRC Cambridge Stem Cell Institute) for her expertise and advice on the TaqMan Array. J.B. wishes to thank Dr. Rachel G. Hoffman (King's College, University of Cambridge) for unwavering support and inspiring discussions.

This work was supported by British Heart Foundation (BHF) award NH/11/1/28922, UK Medical Research Council and BHF Grant G1000847 (S.S.) and the Cambridge Hospitals National Institute for Health Research Biomedical Research Centre funding (S.S.). J.B. was supported by a Cambridge NIHR BRC Cardiovascular Clinical Research Fellowship and subsequently by a BHF PhD Studentship (FS/13/65/30441). L.L. was supported by an MRC award (UK Medical Research Council) and a BHF grant (G1000847). C.C. is supported by the Independent Fellowship from the Institute of Molecular and Cell Biology, Singapore. W.B. is on a BHF PhD studentship FS/11/77/29327. D.I. is on a University of Cambridge Commonwealth Scholarship. L.G. is supported by BHF award RM/l3/3/30159. S.S. is also supported by BHF award FS/13/29/30024.

Acknowledgements: This work was supported by the British Heart Foundation (BHF), the UK Medical Research Council (MRC) and the Cambridge Hospitals National Institute for Health Research Biomedical Research Centre funding.

References

1. Kumar AH, Caplice NM. Clinical potential of adult vascular progenitor cells. Arterioscler Thromb Vasc Biol. 2010; 30(6):1080–7. [PubMed: 20453166]
2. Gaengel K, Genove G, Armulik A, Betsholtz C. Endothelial-mural cell signaling in vascular development and angiogenesis. Arteriosclerosis, thrombosis, and vascular biology. 2009; 29(5): 630–8.
3. Lindahl P, Johansson BR, Leveen P, Betsholtz C. Pericyte loss and microaneurysm formation in PDGF-B-deficient mice. Science. 1997; 277(5323):242–5. [PubMed: 9211853]
4. Andrae J, Gallini R, Betsholtz C. Role of platelet-derived growth factors in physiology and medicine. Genes & development. 2008; 22(10):1276–312. [PubMed: 18483217]
5. Hellstrom M, Gerhardt H, Kalen M, Li X, Eriksson U, Wolburg H, et al. Lack of pericytes leads to endothelial hyperplasia and abnormal vascular morphogenesis. The Journal of cell biology. 2001; 153(3):543–53. [PubMed: 11331305]

6. Jain RK. Molecular regulation of vessel maturation. Nat Med. 2003; 9(6):685–93. [PubMed: 12778167]
7. Carmeliet P. Angiogenesis in health and disease. Nat Med. 2003; 9(6):653–60. [PubMed: 12778163]
8. Majesky MW. Developmental basis of vascular smooth muscle diversity. Arteriosclerosis thrombosis and vascular biology. 2007; 27(6):1248–58.
9. Topouzis S, Majesky MW. Smooth Muscle Lineage Diversity in the Chick Embryo. Developmental biology. 1996; 178(2):430–45.
10. Topouzis S, Majesky MW. Smooth muscle lineage diversity in the chick embryo. Two types of aortic smooth muscle cell differ in growth and receptor-mediated transcriptional responses to transforming growth factor-beta. Developmental biology. 1996; 178(2):430–45.
11. Rosenquist TH, Kirby ML, van Mierop LH. Solitary aortic arch artery. A result of surgical ablation of cardiac neural crest and nodose placode in the avian embryo. Circulation. 1989; 80(5):1469–75. [PubMed: 2805278]
12. Cheung C, Bernardo AS, Trotter MW, Pedersen RA, Sinha S. Generation of human vascular smooth muscle subtypes provides insight into embryological origin-dependent disease susceptibility. Nature biotechnology. 2012; 30(2):165–73.
13. Brons IG, Smithers LE, Trotter MW, Rugg-Gunn P, Sun B, Chuva de Sousa Lopes SM, et al. Derivation of pluripotent epiblast stem cells from mammalian embryos. Nature. 2007; 448(7150): 191–5. [PubMed: 17597762]
14. Cheung C, Bernardo AS, Pedersen RA, Sinha S. Directed differentiation of embryonic origin-specific vascular smooth muscle subtypes from human pluripotent stem cells. Nature protocols. 2014; 9(4):929–38. [PubMed: 24675733]
15. Laflamme MA, Chen KY, Naumova AV, Muskheli V, Fugate JA, Dupras SK, et al. Cardiomyocytes derived from human embryonic stem cells in pro-survival factors enhance function of infarcted rat hearts. Nature biotechnology. 2007; 25(9):1015–24.
16. Shiba Y, Fernandes S, Zhu WZ, Filice D, Muskheli V, Kim J, et al. Human ES-cell-derived cardiomyocytes electrically couple and suppress arrhythmias in injured hearts. Nature. 2012; 489(7415):322–5. [PubMed: 22864415]
17. Chong JJ, Yang X, Don CW, Minami E, Liu YW, Weyers JJ, et al. Human embryonic-stem-cell-derived cardiomyocytes regenerate non-human primate hearts. Nature. 2014
18. Folkman J, Hochberg M. Self-regulation of growth in three dimensions. The Journal of experimental medicine. 1973; 138(4):745–53. [PubMed: 4744009]
19. Zimmermann WH, Melnychenko I, Wasmeier G, Didie M, Naito H, Nixdorff U, et al. Engineered heart tissue grafts improve systolic and diastolic function in infarcted rat hearts. Nature medicine. 2006; 12(4):452–8.
20. Dvir T, Kedem A, Ruvinov E, Levy O, Freeman I, Landa N, et al. Prevascularization of cardiac patch on the omentum improves its therapeutic outcome. Proceedings of the National Academy of Sciences of the United States of America. 2009; 106(35):14990–5. [PubMed: 19706385]
21. Sekine H, Shimizu T, Sakaguchi K, Dobashi I, Wada M, Yamato M, et al. In vitro fabrication of functional three-dimensional tissues with perfusable blood vessels. Nature communications. 2013; 4:1399.
22. Que J, Wilm B, Hasegawa H, Wang F, Bader D, Hogan BL. Mesothelium contributes to vascular smooth muscle and mesenchyme during lung development. Proceedings of the National Academy of Sciences of the United States of America. 2008; 105(43):16626–30. [PubMed: 18922767]
23. Asahina K, Zhou B, Pu WT, Tsukamoto H. Septum transversum-derived mesothelium gives rise to hepatic stellate cells and perivascular mesenchymal cells in developing mouse liver. Hepatology (Baltimore, Md). 2011; 53(3):983–95.
24. Wilm B, Ipenberg A, Hastie ND, Burch JB, Bader DM. The serosal mesothelium is a major source of smooth muscle cells of the gut vasculature. Development (Cambridge, England). 2005; 132(23): 5317–28.
25. Dettman RW, Denetclaw W Jr, Ordahl CP, Bristow J. Common epicardial origin of coronary vascular smooth muscle, perivascular fibroblasts, and intermyocardial fibroblasts in the avian heart. Developmental biology. 1998; 193(2):169–81. [PubMed: 9473322]

26. Trembley MA, Velasquez LS, de Mesy Bentley KL, Small EM. Myocardin-related transcription factors control the motility of epicardium-derived cells and the maturation of coronary vessels. Development (Cambridge, England). 2015; 142(1):21–30.
27. Etchevers HC, Vincent C, Le Douarin NM, Couly GF. The cephalic neural crest provides pericytes and smooth muscle cells to all blood vessels of the face and forebrain. Development (Cambridge, England). 2001; 128(7):1059–68.
28. Foster K, Sheridan J, Veiga-Fernandes H, Roderick K, Pachnis V, Adams R, et al. Contribution of neural crest-derived cells in the embryonic and adult thymus. Journal of immunology (Baltimore, Md : 1950). 2008; 180(5):3183–9.
29. Owens AP 3rd, Subramanian V, Moorleghen JJ, Guo Z, McNamara CA, Cassis LA, et al. Angiotensin II induces a region-specific hyperplasia of the ascending aorta through regulation of inhibitor of differentiation 3. Circulation research. 2010; 106(3):611–9. [PubMed: 20019328]
30. Ota T, Ota K, Jono H, Fujimori H, Ueda M, Shinriki S, et al. Midkine expression in malignant salivary gland tumors and its role in tumor angiogenesis. Oral oncology. 2010; 46(9):657–61. [PubMed: 20637680]
31. Ruan M, Ji T, Wu Z, Zhou J, Zhang C. Evaluation of expression of midkine in oral squamous cell carcinoma and its correlation with tumour angiogenesis. International journal of oral and maxillofacial surgery. 2007; 36(2):159–64. [PubMed: 17110085]
32. Choudhuri R, Zhang HT, Donnini S, Ziche M, Bicknell R. An angiogenic role for the neurokines midkine and pleiotrophin in tumorigenesis. Cancer research. 1997; 57(9):1814–9. [PubMed: 9135027]
33. O'Brien T, Cranston D, Fuggle S, Bicknell R, Harris AL. The angiogenic factor midkine is expressed in bladder cancer, and overexpression correlates with a poor outcome in patients with invasive cancers. Cancer research. 1996; 56(11):2515–8. [PubMed: 8653688]
34. Salama RH, Muramatsu H, Zou P, Okayama M, Muramatsu T. Midkine, a heparin-binding growth factor, produced by the host enhances metastasis of Lewis lung carcinoma cells. Cancer letters. 2006; 233(1):16–20. [PubMed: 15878231]
35. Kishida S, Mu P, Miyakawa S, Fujiwara M, Abe T, Sakamoto K, et al. Midkine promotes neuroblastoma through Notch2 signaling. Cancer research. 2013; 73(4):1318–27. [PubMed: 23243020]
36. Fukui S, Kitagawa-Sakakida S, Kawamata S, Matsumiya G, Kawaguchi N, Matsuura N, et al. Therapeutic effect of midkine on cardiac remodeling in infarcted rat hearts. The Annals of thoracic surgery. 2008; 85(2):562–70. [PubMed: 18222265]
37. Sumida A, Horiba M, Ishiguro H, Takenaka H, Ueda N, Ooboshi H, et al. Midkine gene transfer after myocardial infarction in rats prevents remodelling and ameliorates cardiac dysfunction. Cardiovascular research. 2010; 86(1):113–21. [PubMed: 19969622]
38. Gerhardt H, Golding M, Fruttiger M, Ruhrberg C, Lundkvist A, Abramsson A, et al. VEGF guides angiogenic sprouting utilizing endothelial tip cell filopodia. The Journal of cell biology. 2003; 161(6):1163–77. [PubMed: 12810700]
39. Tammela T, Zarkada G, Wallgard E, Murtomaki A, Suchting S, Wirzenius M, et al. Blocking VEGFR-3 suppresses angiogenic sprouting and vascular network formation. Nature. 2008; 454(7204):656–60. [PubMed: 18594512]
40. Noguera-Troise I, Daly C, Papadopoulos NJ, Coetzee S, Boland P, Gale NW, et al. Blockade of Dll4 inhibits tumour growth by promoting non-productive angiogenesis. Nature. 2006; 444(7122): 1032–7. [PubMed: 17183313]
41. Ridgway J, Zhang G, Wu Y, Stawicki S, Liang WC, Chanthery Y, et al. Inhibition of Dll4 signalling inhibits tumour growth by deregulating angiogenesis. Nature. 2006; 444(7122):1083–7. [PubMed: 17183323]
42. Siekmann AF, Lawson ND. Notch signalling limits angiogenic cell behaviour in developing zebrafish arteries. Nature. 2007; 445(7129):781–4. [PubMed: 17259972]
43. Leslie JD, Ariza-McNaughton L, Bermange AL, McAdow R, Johnson SL, Lewis J. Endothelial signalling by the Notch ligand Delta-like 4 restricts angiogenesis. Development (Cambridge, England). 2007; 134(5):839–44.

44. Patsch C, Challet-Meylan L, Thoma EC, Urich E, Heckel T, O'Sullivan JF, et al. Generation of vascular endothelial and smooth muscle cells from human pluripotent stem cells. Nature cell biology. 2015; 17(8):994–1003. [PubMed: 26214132]
45. Orlova VV, Drabsch Y, Freund C, Petrus-Reurer S, van den Hil FE, Muenthaisong S, et al. Functionality of endothelial cells and pericytes from human pluripotent stem cells demonstrated in cultured vascular plexus and zebrafish xenografts. Arteriosclerosis, thrombosis, and vascular biology. 2014; 34(1):177–86.
46. Potus F, Ruffenach G, Dahou A, Thebault C, Breuils-Bonnet S, Tremblay E, et al. Downregulation of miR-126 Contributes to the Failing Right Ventricle in Pulmonary Arterial Hypertension. Circulation. 2015
47. Esser JS, Rahner S, Deckler M, Bode C, Patterson C, Moser M. Fibroblast growth factor signaling pathway in endothelial cells is activated by BMPER to promote angiogenesis. Arteriosclerosis thrombosis and vascular biology. 2015; 35(2):358–67.
48. Hassel D, Cheng P, White MP, Ivey KN, Kroll J, Augustin HG, et al. MicroRNA-10 regulates the angiogenic behavior of zebrafish and human endothelial cells by promoting vascular endothelial growth factor signaling. Circulation research. 2012; 111(11):1421–33. [PubMed: 22955733]
49. Nolan DJ, Ginsberg M, Israely E, Palikuqi B, Poulos MG, James D, et al. Molecular signatures of tissue-specific microvascular endothelial cell heterogeneity in organ maintenance and regeneration. Developmental cell. 2013; 26(2):204–19. [PubMed: 23871589]

Europe PMC Funders Author Manuscripts

Europe PMC Funders Author Manuscripts

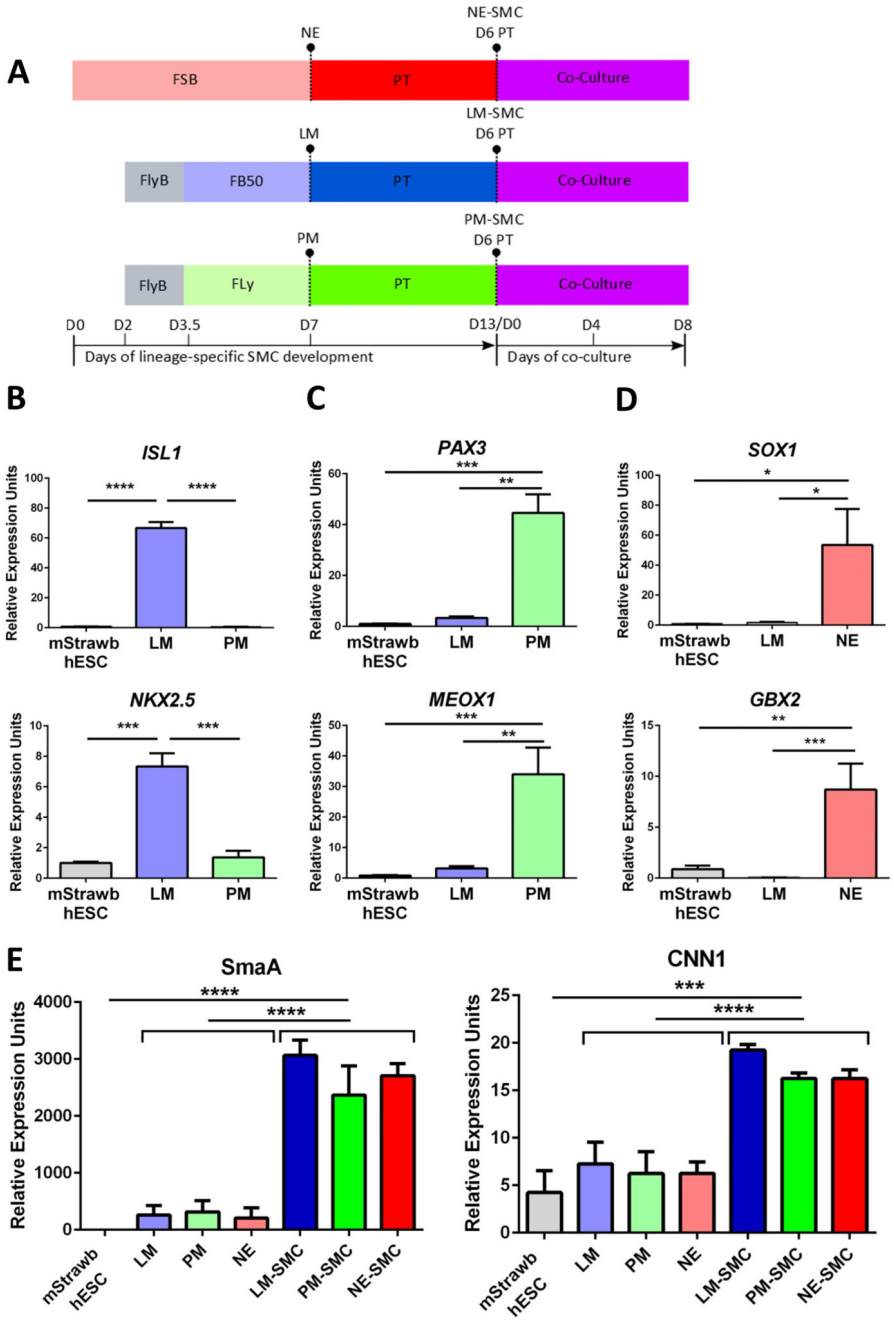

Fig. 1. Generation of embryonic origin specific SMC populations for a 3D co-culture model.

(A) Schematic representation of the *in vitro* differentiation of embryonic origin-specific SMCs. Neuroectoderm (NE) was differentiated from hESCs using FGF2+SB431542 (FSB) treatment for 7 days. hESCs were also differentiated to early mesoderm in FGF2+LY294002+BMP4 (FlyB) for 36 hr and subsequently to lateral mesoderm (LM) in FGF2+BMP4 (FB50) or paraxial mesoderm (PM) in FGF2+LY294002 (Fly) for 3.5 days. For further differentiation into vascular SMCs, each of the three intermediate lineages was subjected to PDGF-BB+TGF-β (PT) treatment for 6 days, then co-cultured with HUVECs.

(B-D) Validation of the identity of the intermediate lineages, LM, PM and NE respectively, by qRT-PCR analysis of lineage specific markers (n=3). *(E)* SMC marker expression in D6 PT treated SMCs by qRT-PCR (*p<0,05, **p<0,01, ***p<0,001, ****p<0.0001, n=3 independent biological replicates).

Europe PMC Funders Author Manuscripts

Europe PMC Funders Author Manuscripts

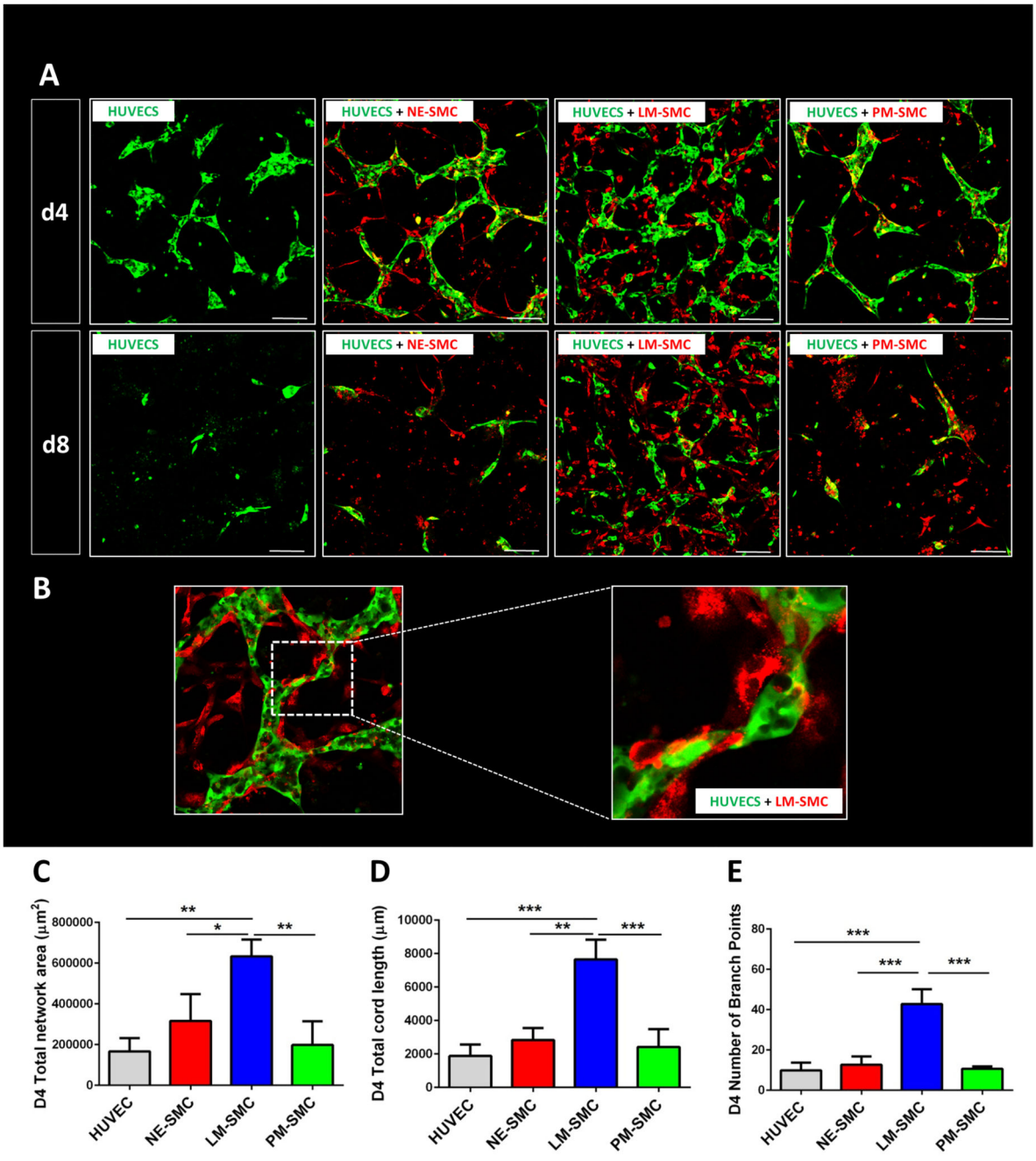

Fig. 2. LM-derived SMCs best support HUVEC network formation in a 3D co-culture model.

(A) Confocal images of HUVEC (green) co-cultures with the three respective SMC types (red) on day 4 and day 8 of the co-culture protocol. *(B)* SMCs provide physical support to developing networks, wrapping around endothelial network. (C) Quantification of total network area in µm2. *(D)* Quantification of total cord length. *(E)* Quantification of number of branch points. Quantitative data is shown for day 4 of the co-culture (*p<0,05, **p<0,01, ***p<0,001, n=3 independent biological triplicates, scale bars= 100 µm).

Europe PMC Funders Author Manuscripts

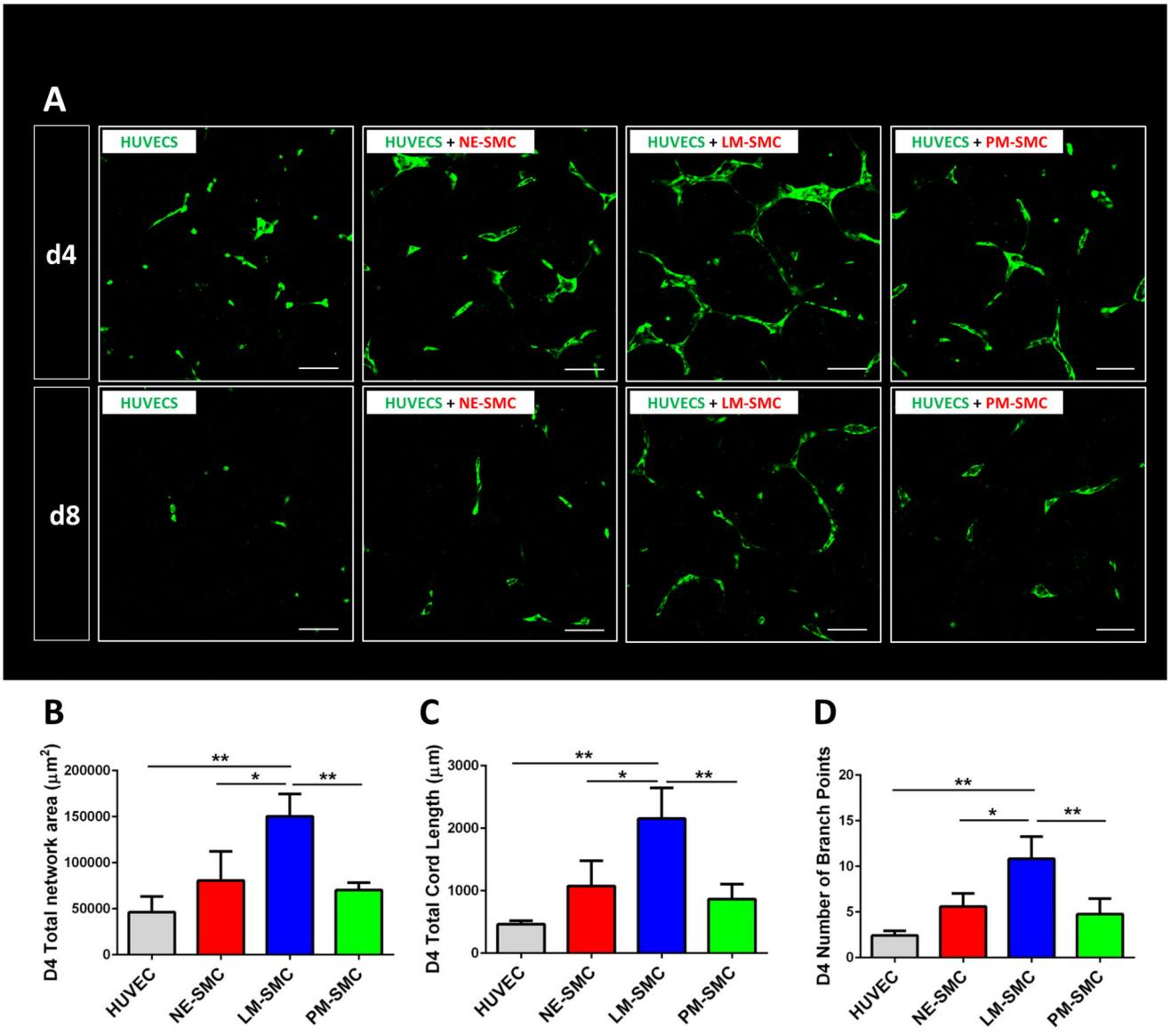

Fig. 3. Paracrine effects of lineage-specific SMCs on HUVEC networks.

HUVECs were exposed to supernatant conditioned by lineage specific SMCs (as depicted in fig. S4B). *(A)* Confocal images of paracrine co-cultures taken on day 4 and day 8 of the protocol. *(B)* Quantification of total network area in µm^2. *(C)* Quantification of total cord length. (*D*) Quantification of number of branch points. Quantitative data is shown for day 4 of the co-culture (*p<0,05, **p<0,01, ***p<0,001, n=3 independent biological replicates, scale bars= 100 µm).

Europe PMC Funders Author Manuscripts

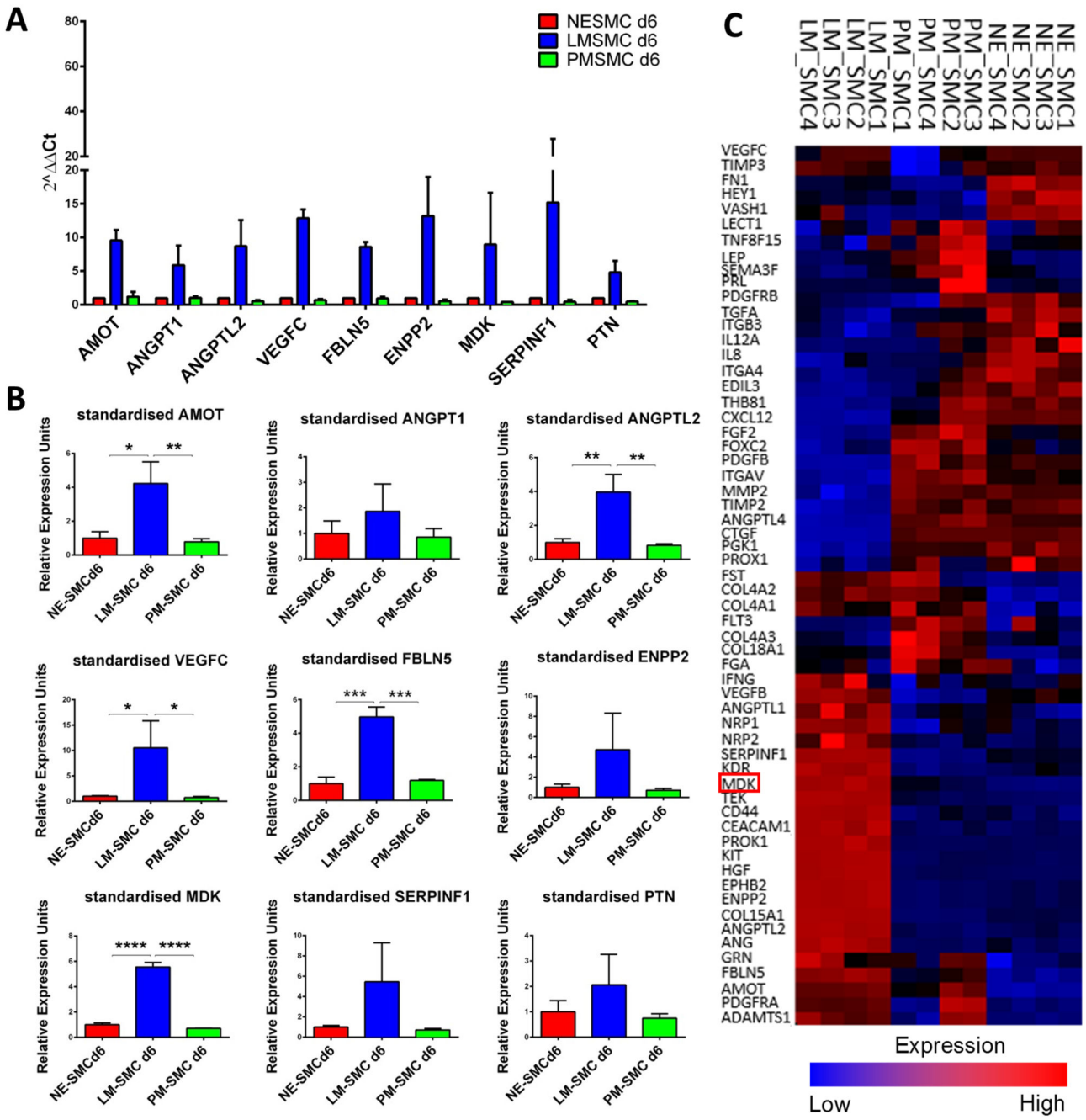

Fig. 4. Putative mediators of network formation identified by TaqMan© Array and microarray.

(A) Candidate genes differentially up-regulated in LM-derived SMCs as per Taqman Array Human angiogenesis panel. Transfection of scrambled siRNA (siScr) was used as negative control. *(B)* Validation of the TaqMan© Array by qRT-PCR. *(C)* Lineage-specific gene signatures of the three embryonic origin specific SMC lines per microarray. MDK is highlighted in red. Red (upregulation) and blue (downregulation) reflect expression from the mean across all samples (*p<0,05, **p<0,01, ***p<0,001, n=3 independent biological replicates).

Europe PMC Funders Author Manuscripts

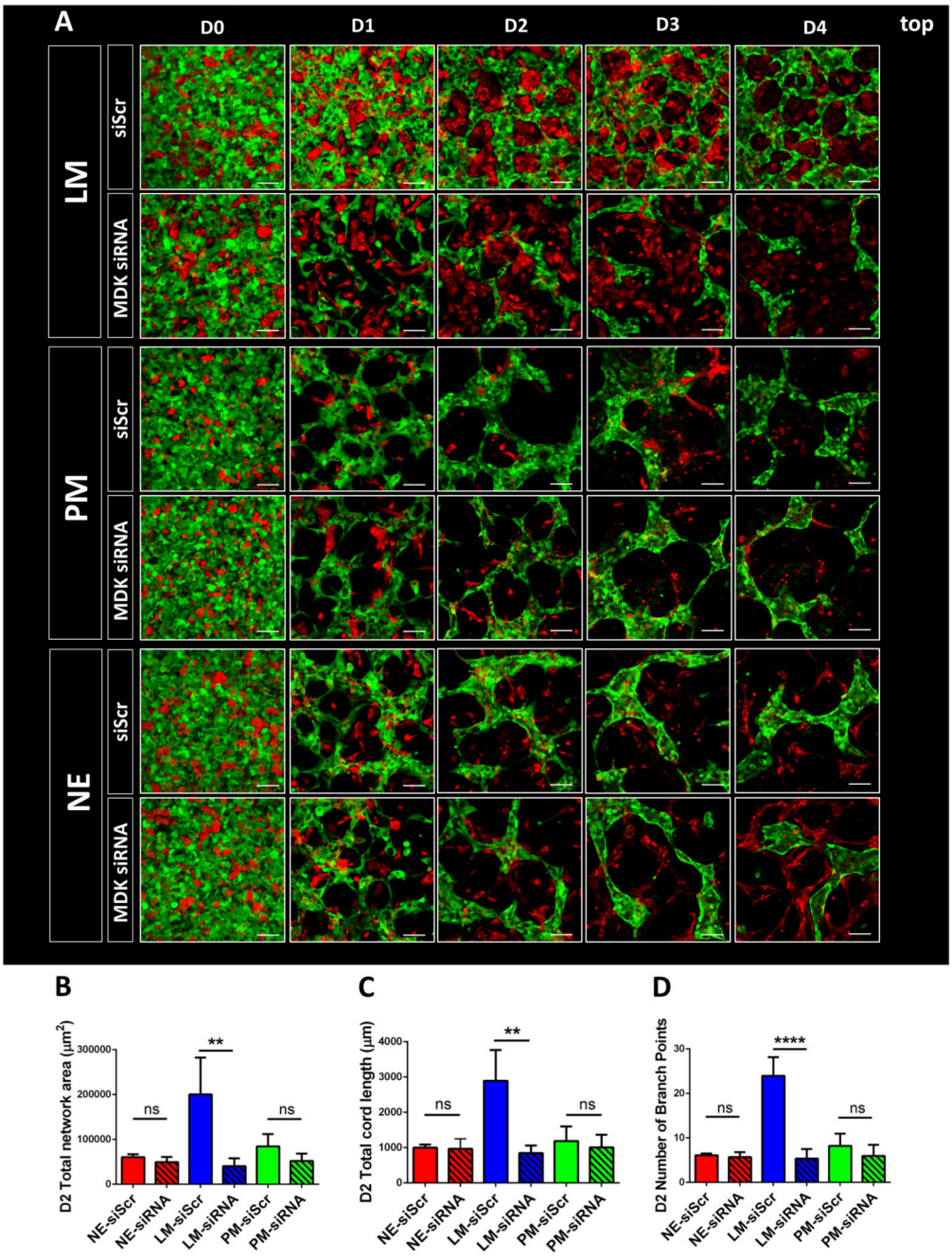

Fig. 5. siRNA-mediated knockdown of MDK in 3D co-cultures.

(A) Effect of MDK knockdown in SMCs on HUVEC network formation in 3D co-culture as per confocal microscopy over a 4 day timeline. Transfection of scrambled siRNA (siScr) was used as negative control. *(B)* Quantification of the effect of MDK siRNA-mediated knockdown on total network area in co-cultures of the three SMC lineages on day 2. *(C)* Quantification of total cord length in co-cultures containing MDK-siRNA treated SMCs on day 2. *(D)* Quantification of the effect of MDK siRNA-mediated knockdown on the number

of branch points in co-cultures of the three SMC lineages on day 2. (*p<0,05, **p<0,01, ***p<0,001, n=3 independent biological replicates, scale bars= 100 μm).

Europe PMC Funders Author Manuscripts

Europe PMC Funders Author Manuscripts

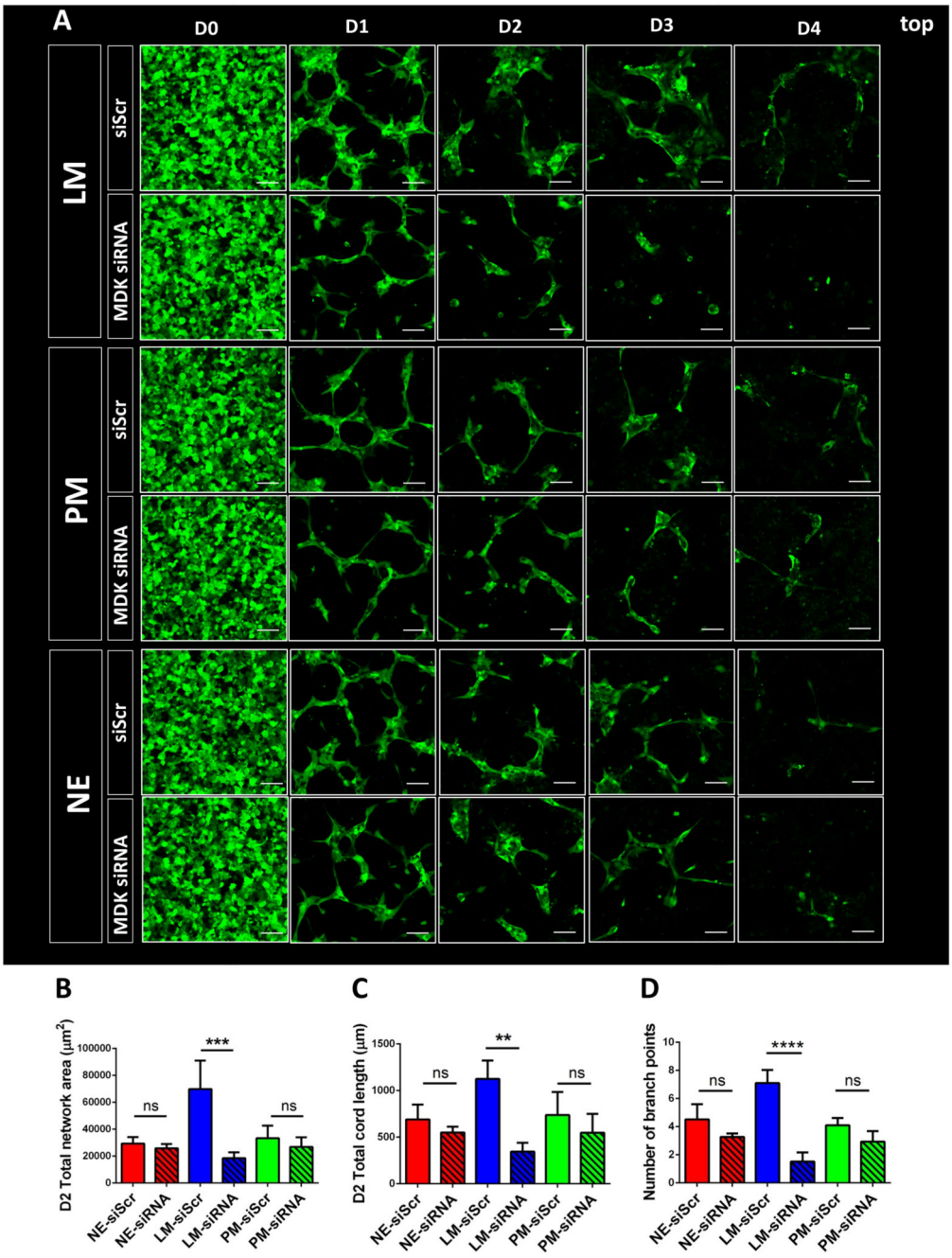

Fig. 6. siRNA-mediated knockdown of MDK in 3D paracrine assays.

(A) Effect of MDK knockdown in SMC on HUVEC network formation in 3D paracrine co-culture as per confocal microscopy over a 4 day timeline. *(B)* Quantification of the effect of MDK siRNA-mediated knockdown on total HUVEC network area in co-cultures with the three SMC lineages on day 2. *(C)* Quantification of total cord length in co-cultures containing MDK-siRNA treated SMCs on day 2. *(D)* Quantification of the effect of MDK siRNA-mediated knockdown on the number of branch points in co-cultures of the three

SMC lineages on day 2. (*p<0,05, **p<0,01, ***p<0,001, n=3 independent biological replicates, scale bars= 100 μm).

Europe PMC Funders Author Manuscripts

Europe PMC Funders Author Manuscripts

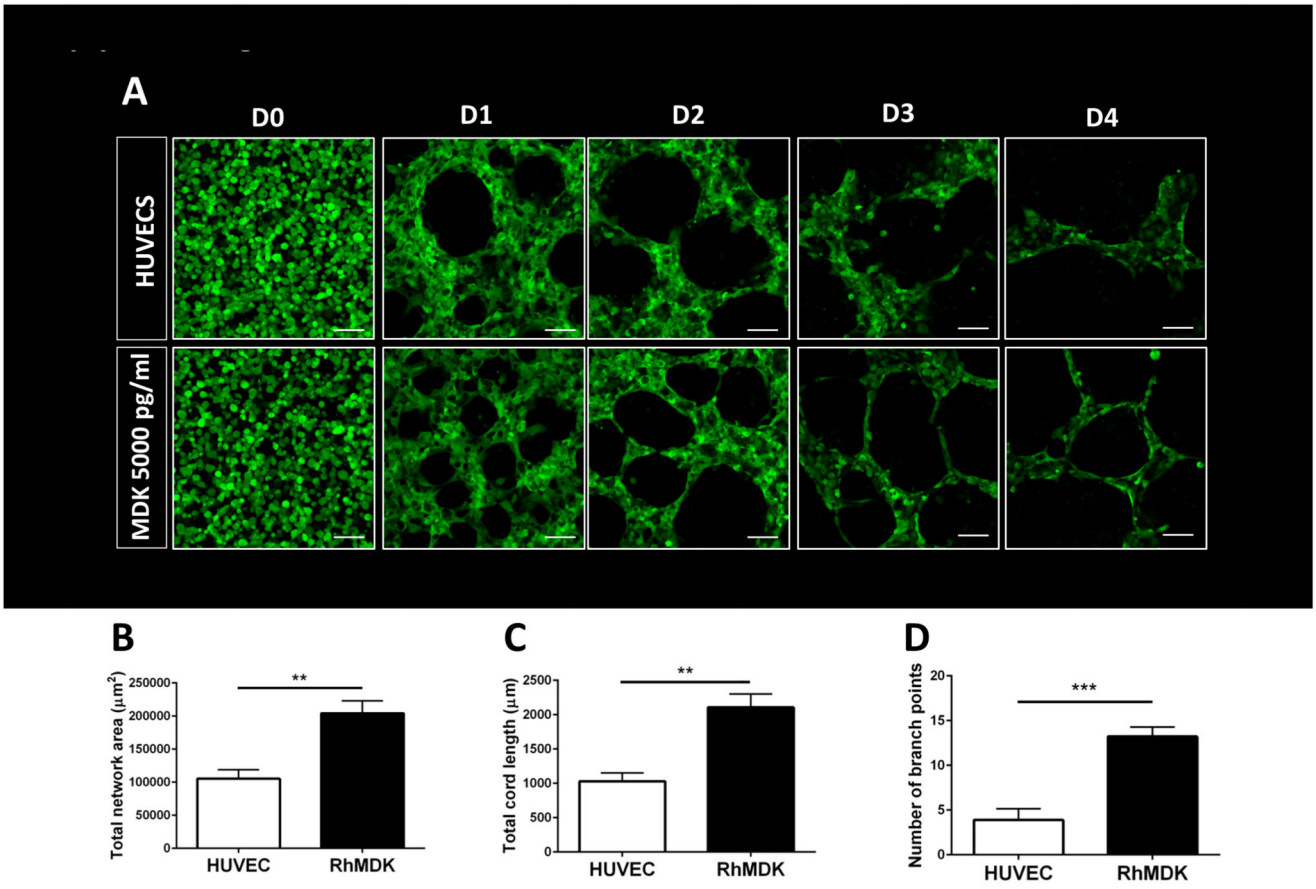

Fig. 7. Addition of recombinant MDK in 3D HUVEC mono-cultures.

(A) Effect of recombinant MDK on HUVEC network formation in 3D HUVEC monocultures as per confocal microscopy over a 4 day timeline. Quantification of the effect of recombinant MDK (B) on total network area in HUVEC monocultures on day 2; (C) on total cord length on day 2; and (D) on the number of branch points on day 2 (*p<0,05, **p<0,01, ***p<0,001, n=3 independent biological replicates, scale bars= 100 µm).